

Hadron collisions at ultrahigh energies: Black disk or resonant disk modes?

V. V. Anisovich and V. A. Nikonov

*National Research Centre “Kurchatov Institute”, Petersburg Nuclear Physics Institute,
Gatchina 188300, Russia*

J. Nyiri

*Institute for Particle and Nuclear Physics, Wigner Research Centre for Physics, Budapest 1121, Hungary
(Received 27 August 2014; published 3 October 2014)*

The analysis of current ultrahigh energy data for hadronic total cross sections and diffractive scattering cross sections points to a steady growth of the optical density with energy for elastic scattering amplitudes in the impact parameter space, b . At LHC energy the profile function of the pp -scattering amplitude, $T(b)$, reaches the black disk limit at small b . Two scenarios are possible at larger energies, $\sqrt{s} \gtrsim 100$ TeV. First, the profile function gets frozen in the black disk limit, $T(b) \simeq 1$, while the radius of the black disk $R_{\text{black disk}}$ is increasing with $\ln s$, providing $\sigma_{\text{tot}} \sim \ln^2 s$, $\sigma_{\text{el}} \sim \ln^2 s$, $\sigma_{\text{inel}} \sim \ln^2 s$. In another scenario the profile function continues to grow at $\sqrt{s} \gtrsim 100$ TeV approaching the maximal value, $T(b) \simeq 2$, that means the resonant disk mode. We discuss features of the resonant disk mode when the disk radius, $R_{\text{resonant disk}}$, increases providing the growth of the total and elastic cross sections $\sigma_{\text{tot}} \sim \ln^2 s$, $\sigma_{\text{el}} \sim \ln^2 s$, but a more slow increase of inelastic cross section, $\sigma_{\text{inel}} \sim \ln s$.

DOI: 10.1103/PhysRevD.90.074005

PACS numbers: 13.85.Lg, 13.85.-t, 13.75.Cs, 14.20.Dh

I. INTRODUCTION

Recent data [1,2] definitely confirm the previous observations [3], namely, that the total cross sections increase steadily with energy ($\sigma_{\text{tot}} \sim \ln^n s$ as $1 \lesssim n \lesssim 2$); the steady growth is observed for σ_{el} and σ_{inel} , while the ratio $\text{Re}A_{\text{el}}/\text{Im}A_{\text{el}}$ is small and probably decreases slowly.

Already the first indications of the cross sections growth [4] gave start to corresponding models with the supercritical pomeron [5,6]. The concept of the power growth of cross sections ($\sigma_{\text{tot}} \sim s^\Delta$ with $\Delta \simeq 0.08$) became widely accepted in the 1980 s [7,8] and was discussed till now [9] (let us note that exceeding of the Froissart bound [10] does not violate necessarily the general constraints [11]).

It was shown in Ref. [12–14] that the power-type growth of scattering amplitudes is dumped to $\ln^2 s$ type within the s -channel unitarization. The black disk picture with the $\ln^2 s$ growth of the σ_{tot} and σ_{el} at ultrahigh energies was suggested in the Dakhno–Nikonov model [15]. The model can be considered as a realization of the Good–Walker eikonal approach [16] for a continuous set of channels. Presently, the black disk mode for hadron collisions at ultrahigh energies is discussed extensively; see, for example, Refs. [17–25].

The black disk mode is usually discussed in terms of the optical density for the elastic scattering amplitude. For the asymptotic regime such a presentation was carried out in Refs. [26,27]: the cross sections $\sigma_{\text{tot}}(pp)$, $\sigma_{\text{el}}(pp)$, $\sigma_{\text{inel}}(pp)$ demonstrate a maximal growth, $\sim \ln^2 s$, while diffractive dissociation cross sections $\sigma_D(pp)$, $\sigma_{DD}(pp)$ give a slower growth, $\sim \ln s$.

For the calculation of screening corrections in inelastic diffractive processes at ultrahigh energies [28] the K -matrix technique is more preferable. The K -matrix function $-iK(b)$ in the pre-LHC region increases with energy being mainly concentrated at $b < 1$ fm. The black disk regime for the K -matrix function means its “freezing,” $-iK(b) \rightarrow 1$, in the disk area. If the growth of the $-iK(b)$ continues with increasing energy, the interaction area turns into a resonant disk. In this case asymptotically $\sigma_{\text{tot}}(pp) \sim \ln^2 s$, $\sigma_{\text{el}}(pp) \sim \ln^2 s$ with $[\sigma_{\text{el}}(pp)/\sigma_{\text{tot}}(pp)]_{s \rightarrow \infty} \rightarrow 1$; the resonant disk area is surrounded by a black border band that provides $\sigma_{\text{inel}}(pp) \sim \ln s$, $\sigma_D(pp) \sim \ln s$, $\sigma_{DD}(pp) \sim \ln s$.

In the present paper we perform a comparative analysis of predictions for ultrahigh energy diffractive processes in the framework of these two scenarios. It is definitely seen that the data at $\sqrt{s} \sim 10$ TeV are not sensitive to the versions of the disk; the initial stages are similar in both modes. Distinctions are seen at $\sqrt{s} \sim 10^3\text{--}10^4$ TeV. Apparently, the study and interpretation of the cosmic ray data at such energies are the problems on the agenda.

**II. SCATTERING AMPLITUDE IN THE
IMPACT PARAMETER SPACE AND
THE K-MATRIX REPRESENTATION
FOR ULTRAHIGH ENERGY**

In the impact parameter space the profile function $T(b)$ is determined at high energies as

$$\sigma_{\text{tot}} = 2 \int d^2b T(b),$$

$$4\pi \frac{d\sigma_{\text{el}}}{d\mathbf{q}_{\perp}^2} = |A_{\text{el}}(\mathbf{q}_{\perp}^2)|^2, \quad A_{\text{el}}(\mathbf{q}_{\perp}^2) = i \int d^2b e^{i\mathbf{q}_{\perp} \cdot \mathbf{b}} T(b),$$

$$T(b) = 1 - \eta(b) e^{2i\delta(b)} = 1 - e^{-\frac{1}{2}\chi(b)} = \frac{-2iK(b)}{1 - iK(b)}; \quad (1)$$

here $A_{\text{el}}(\mathbf{q}_{\perp}^2)$ is the elastic scattering amplitude. The profile function can be presented either in the standard form using the inelasticity parameter $\eta(b)$ and the phase shift $\delta(b)$ or in terms of the optical density $\chi(b)$ and the K -matrix function $K(b)$. The K -matrix approach is based on the separation of the elastic rescatterings in the intermediate states; the function $K(b)$ includes only the multiparticle states thus being complex valued. The small value of the $\text{Re}A_{\text{el}}/\text{Im}A_{\text{el}}$ tells that $K(b)$ is dominantly imaginary.

A. Black disk limit in terms of the Dakhno–Nikonov model

The Dakhno–Nikonov model [15] provides us with a representative example of application of the optical density technique for the consideration of pp^{\pm} collisions at ultra-high energies when $\ln s \gg 1$. In the model the black disk is formed by the low density pomeron cloud, and rescatterings are described within the eikonal approach. The scattering amplitude $AB \rightarrow AB$ reads

$$A_{AB \rightarrow AB}(\mathbf{q}^2) = i \int d^2b e^{i\mathbf{q} \cdot \mathbf{b}} \int dr' \varphi_A^2(r') dr'' \varphi_B^2(r'') \times \left[1 - \exp\left(-\frac{1}{2}\chi_{AB}(r', r'', \mathbf{b})\right) \right], \quad (2)$$

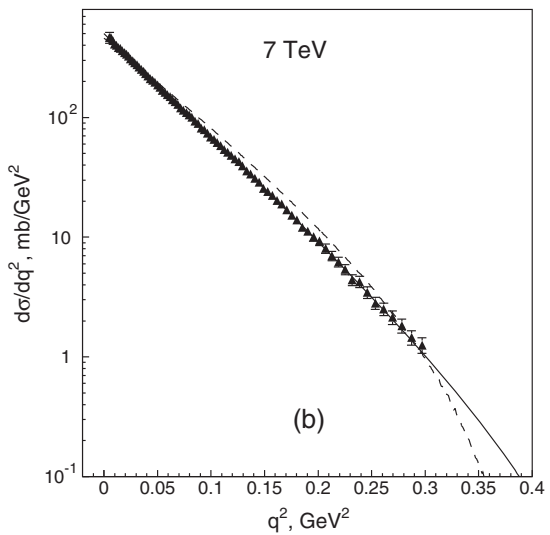
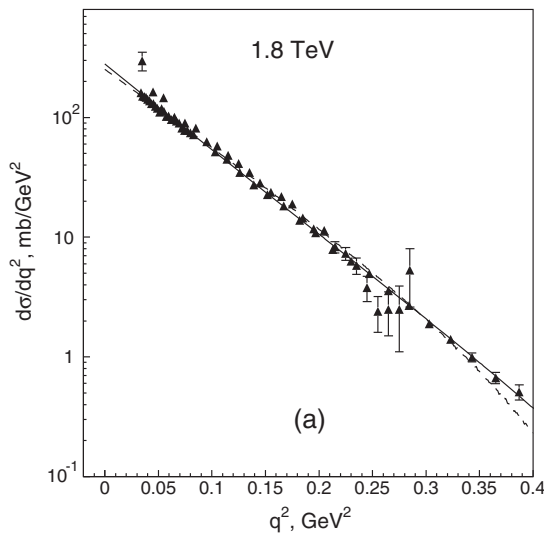


FIG. 1. (a,b) Differential cross sections $d\sigma_{\text{el}}/d\mathbf{q}_{\perp}^2$ at $\sqrt{s} = 1.8, 7.0$ TeV and their description within the black disk mode (dashed lines) and the resonant disk mode (solid lines).

where $dr\varphi_A^2(r)$, $dr\varphi_B^2(r)$ are the quark densities of the colliding hadrons in the impact parameter space. Proton and pion quark densities can be determined using the corresponding form factors. The optical density $\chi_{AB}(r', r'', \mathbf{b})$ depends on parameters of the t -channel interaction.

The behavior of amplitudes at ultrahigh energies is determined by leading complex- j singularities, in the Dakhno–Nikonov model, that are leading and next-to-leading pomerons with trajectories $\alpha(\mathbf{q}^2) \simeq 1 + \Delta - \alpha' \mathbf{q}^2$. The fit of Refs. [22,26] gives

Parameters	Leading pole	Next to leading
Δ	0.27	0
α'_p [(GeV) $^{-2}$]	0.13	0.25

In terms of the K -matrix approach the black disk mode means the assumed freezing of the $-iK(b)$ in the interaction area:

$$[-iK(b)]_{\xi \rightarrow \infty} \rightarrow 1 \quad \text{at } b < R_0 \xi,$$

$$[-iK(b)]_{\xi \rightarrow \infty} \rightarrow 0 \quad \text{at } b > R_0 \xi,$$

$$\xi = \ln \frac{s}{s_R}, \quad s_R \simeq 6.4 \times 10^3 \text{ GeV}^2,$$

$$\text{with } R_0 \simeq 2\sqrt{\alpha' \Delta} \simeq 0.08 \text{ fm}. \quad (3)$$

The growth of the radius of the black disk is slow; the small value of R_0 is caused by the large mass of glueballs [29,30] and the effective mass of gluons [31,32].

The black disk mode results in

$$\sigma_{\text{tot}} \simeq 2\pi(R_0 \xi)^2,$$

$$\sigma_{\text{el}} \simeq \pi(R_0 \xi)^2, \quad \sigma_{\text{inel}} \simeq \pi(R_0 \xi)^2. \quad (4)$$

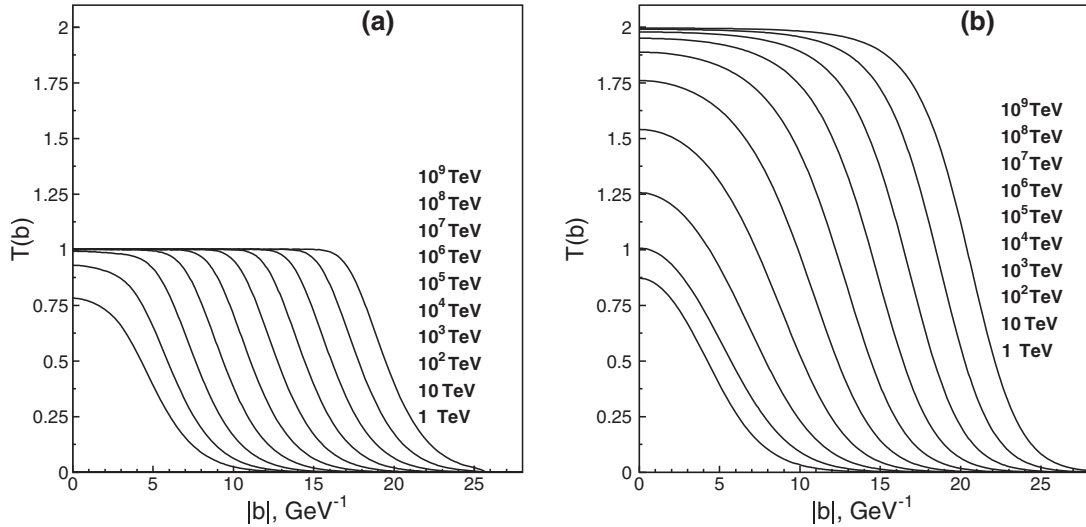


FIG. 2. (a) Profile functions, $T(b)$, from left to right $\sqrt{s} = 1, 10, 10^2, \dots, 10^9$ TeV for the black disk regime ($T(b) \rightarrow 1$) and (b) resonant disk regime ($T(b) \rightarrow 2$). At $\sqrt{s} = 1$ – 10 TeV the profile functions in both modes are nearly the same.

For the black disk radius the corrections of the order of $\ln \xi$ exist $R_{\text{black disk}} \simeq R_0 \xi + \rho \ln \xi$, but they would only become apparent in the Dakhno–Nikonov model at energies of the order of the Planck mass, $\sqrt{s} \sim 10^{17}$ TeV.

B. Resonant disk and K -matrix function

From the data it follows that both $T(b)$ and $-iK(b)$ are increasing with energy, being less than unity. If the eikonal mechanism does not quench the growth, both characteristics cross the black disk limit getting $T(b) > 1$, $-iK(b) > 1$. If $-iK(b) \rightarrow \infty$ at $\ln s \rightarrow \infty$, which corresponds to a growth caused by the supercritical pomeron ($\Delta > 0$), the interaction process gets to the resonant disk mode.

For following the resonant disk switch on, we use the two-pomeron model with parameters providing the description of data at 1.8 and 7 TeV, namely

$$\begin{aligned} -iK(b) &= \int \frac{d^2q}{(2\pi)^2} \exp(-i\mathbf{q}\mathbf{b}) \sum g^2 s^\Delta e^{-(a+\alpha\xi)\mathbf{q}^2} \\ &= \sum \frac{g^2}{4\pi(a+\alpha'\xi)} \exp\left[\Delta\xi - \frac{\mathbf{b}^2}{4(a+\alpha'\xi)}\right], \\ \xi &= \ln \frac{s}{s_0}. \end{aligned} \quad (5)$$

The following parameters are found for the leading and the next-to-leading pomerons:

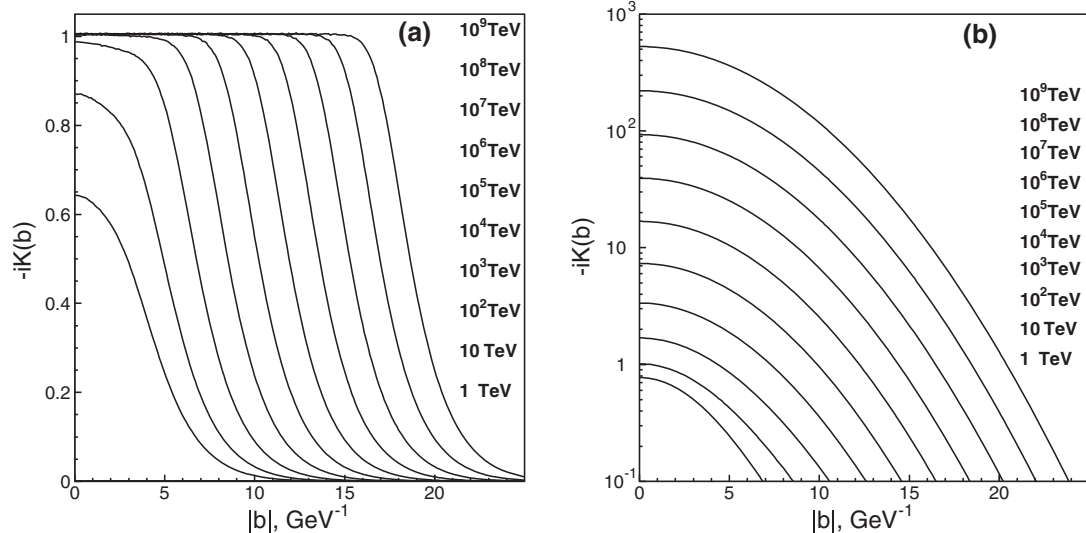


FIG. 3. The K -matrix functions, $-iK(b)$, for (a) the black disk mode ($[-iK(b)]_{\xi \rightarrow \infty} \rightarrow 1$ at $b < R_0 \xi$) and (b) the resonant disk mode ($[-iK(b)]_{\xi \rightarrow \infty} \rightarrow \infty$ at $b < R_0 \xi$).

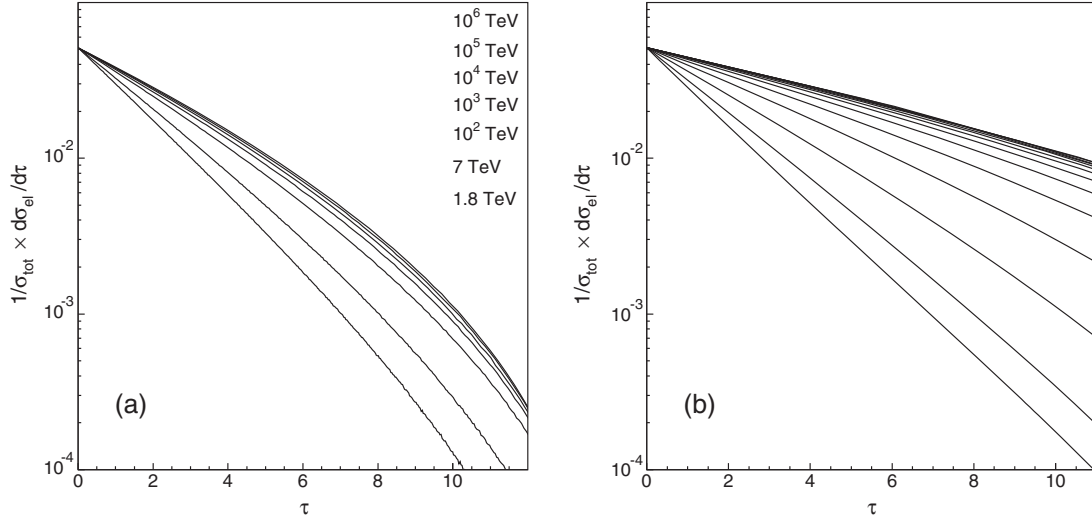


FIG. 4. The black disk (a) and resonant disk (b) modes: the τ dependence of the differential cross sections ($\tau = \sigma_{\text{tot}} \mathbf{q}^2$) for differential cross section, $\frac{1}{\sigma_{\text{tot}}} \frac{d\sigma_{\text{el}}}{d\tau}$. The differential cross sections are similar at $\sqrt{s} = 1.8, 7$ TeV; distinctions are seen at $\sqrt{s} \geq 10^3$ TeV.

Parameters	Leading pole	Next to leading
Δ	0.20	0
α'_p [GeV^{-2}]	0.18	0.14
α [GeV^{-2}]	6.67	2.22
g^2 [mb]	1.74	28.6
s_0 [GeV^2]	1	1

The description of the differential cross sections $d\sigma_{\text{el}}/d\mathbf{q}_\perp^2$ at $\sqrt{s} = 1.8, 7.0$ TeV in the resonant disk mode is demonstrated in Fig. 1. The resonant interaction regime occurs at $b < 2\sqrt{\alpha'}\Delta\xi = R_0\xi$, in this region $T(b) \rightarrow 2$. In terms of the inelasticity parameter and the phase shift it corresponds to $\eta \rightarrow 1$ and $\delta \rightarrow \pi/2$. Cross sections at $\xi \rightarrow \infty$ obey $\sigma_{\text{tot}} \approx 4\pi R_0^2 \xi^2$, $\sigma_{\text{el}}/\sigma_{\text{tot}} \rightarrow 1$, and $\sigma_{\text{inel}} \approx 2\pi R_0 \xi$.

C. Comparative survey of the resonant disk and black disk modes

At the energy $\sqrt{s} \sim 10$ TeV the black cloud fills out the proper hadron domain, the region ≤ 1 fm, and that happens in both modes. It is demonstrated in Figs. 2 and 3: the profile functions $T(b)$ coincide practically in both modes as well as the K functions $-iK(b)$. Correspondingly, τ dependence of the differential cross sections differ here only a little, mainly at $\tau \sim 10$, Fig. 4. The energy behavior of σ_{tot} , σ_{el} , and σ_{inel} coincide also at $\sqrt{s} \sim 1\text{--}100$ TeV in both modes, Fig. 5.

Differences appear at $\sqrt{s} \sim 1000$ TeV: $T(b) \approx 1.5$ at $b \lesssim 0.5$ fm, and the black zone has shifted to $b \approx 1.0\text{--}1.5$ fm, Fig. 3b. With further energy increase the radius of the black band increases as $2\sqrt{\Delta\alpha'}\xi \equiv R_{rd}\xi$. The rate of growth in both modes is determined by the leading singularity, and the fit of the data in the region $\sqrt{s} \sim 1\text{--}10$ TeV gives approximately

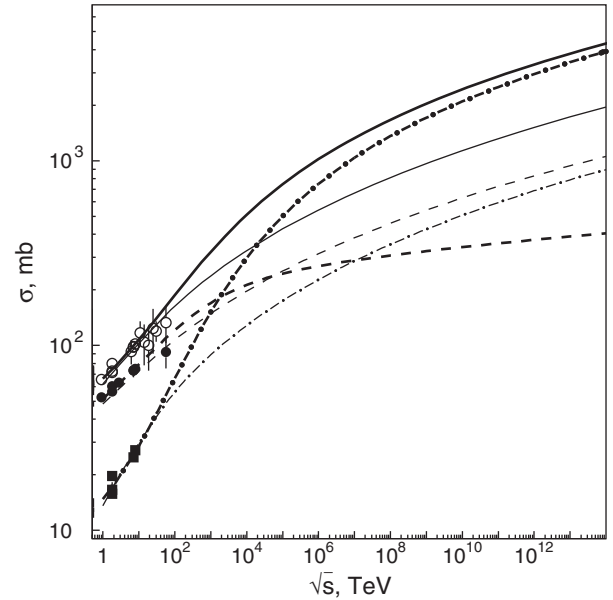


FIG. 5. Total, elastic, and inelastic cross sections for resonant disk (thick lines) and black disk (thin lines) modes: open circles and solid lines are σ_{tot} , squares and dot-dashed lines are σ_{el} , and filled circles and dashed lines are σ_{inel} .

the same values of Δ and α' for both cases, thus providing $R_0 \approx R_{rd}$.

III. CONCLUSION

The interaction of soft gluons largely determines the physics of hadrons. The effective gluons are massive, and their mass is of the order of 1 GeV that is most clearly seen in radiative decays of heavy quarkonia [31,32], $\psi \rightarrow \gamma + \text{hadrons}$ and $\Upsilon \rightarrow \gamma + \text{hadrons}$. The effective gluon mass is determinative both for low energy physics, making possible

to introduce the notion of the constituent quark, and for high energy physics, dictating the rate of the growth of the interaction radius. High energy physics is the physics of large logarithms, $\ln s/s_0 \gg 1$, and the value $\sqrt{s_0} \sim m_{\text{effectivegluon}}$ corresponds to a start of the asymptotic regime at $\sqrt{s} \sim 1$ TeV. However, the initial increments of the measured characteristics such as σ_{tot} , σ_{el} , and σ_{inel} are visually similar, and therefore their behavior in this region does not distinguish between different versions discussed above. A real distinction of modes can appear when the cross section data are discussed at much larger energies, $\sqrt{s} \sim 10^3\text{--}10^4$ TeV.

Cosmic ray data can probably provide an information to fix the asymptotic mode. Another way is to study the diffractive inelastic processes which differ strongly for both considered modes [28].

ACKNOWLEDGMENTS

We thank M. G. Ryskin and A. V. Sarantsev for useful discussions and comments. The work was supported by Russian Foundation for Basic Research in Grant No. RFBR-13-02-00425 and Federal Program of the Russian State in Grant No. RSGSS-4801.2012.2.

-
- [1] G. Latino (TOTEM Collaboration), *EPJ Web Conf.* **49**, 02005 (2013).
- [2] P. Abreu *et al.* (Pierre Auger Collaboration), *Phys. Rev. Lett.* **109**, 062002 (2012).
- [3] UA4 Collaboration, *Phys. Lett.* **147B**, 385 (1984); UA4/2 Collaboration, *Phys. Lett. B* **316**, 448 (1993); UA1 Collaboration, *Phys. Lett.* **128B**, 336 (1983); E710 Collaboration, *Phys. Lett. B* **247**, 127 (1990); CDF Collaboration, *Phys. Rev. D* **50**, 5518 (1994).
- [4] Yu. P. Gorin *et al.*, *Yad. Fiz.* **14**, 998 (1971).
- [5] A. Capella and J. Kaplan, *Phys. Lett.* **52B**, 448 (1974).
- [6] P. E. Volkovitsky, M. A. Lapidus, V. I. Lisin, and K. A. Ter-Martirosyan, *Yad. Fiz.* **24**, 1237 (1976) [*Sov. J. Nucl. Phys.* **24**, 648 (1976)].
- [7] A. Donnachie and P. V. Landshoff, *Nucl. Phys.* **B231**, 189 (1984).
- [8] A. B. Kaidalov and K. A. Ter-Martirosyan, *Yad. Fiz.* **39**, 1545 (1984) [*Sov. J. Nucl. Phys.* **39**, 979 (1984)].
- [9] A. Donnachie and P. V. Landshoff, [arXiv:1112.2485](https://arxiv.org/abs/1112.2485).
- [10] M. Froissart, *Phys. Rev.* **123**, 1053 (1961).
- [11] Y. I. Azimov, *Phys. Rev. D* **84**, 056012 (2011); [arXiv:1208.4304](https://arxiv.org/abs/1208.4304).
- [12] T. K. Gaisser and T. Stanev, *Phys. Lett. B* **219**, 375 (1989).
- [13] M. Block, F. Halzen, and B. Margolis, *Phys. Lett. B* **252**, 481 (1990).
- [14] R. S. Fletcher, *Phys. Rev. D* **46**, 187 (1992).
- [15] L. G. Dakhno and V. A. Nikonov, *Eur. Phys. J. A* **5**, 209 (1999).
- [16] M. L. Good and W. D. Walker, *Phys. Rev.* **120**, 1857 (1960).
- [17] F. Halzen, K. Igi, M. Ishida, and C. S. Kim, *Phys. Rev. D* **85**, 074020 (2012).
- [18] V. Uzhinsky and A. Galoyan, [arXiv:1111.4984v5](https://arxiv.org/abs/1111.4984v5).
- [19] M. G. Ryskin, A. D. Martin, and V. A. Khoze, *Eur. Phys. J. C* **72**, 1937 (2012).
- [20] I. M. Dremin and V. A. Nechitailo, *Phys. Rev. D* **85**, 074009 (2012).
- [21] M. M. Block and F. Halzen, *Phys. Rev. D* **86**, 051504 (2012).
- [22] V. V. Anisovich, K. V. Nikonov, and V. A. Nikonov, *Phys. Rev. D* **88**, 014039 (2013).
- [23] A. Alkin, E. Martynov, O. Kovalenko, and S. M. Troshin, *Phys. Rev. D* **89**, 091501 (2014).
- [24] S. M. Troshin and N. E. Tyurin, *Int. J. Mod. Phys. A* **22**, 4437 (2007); [arXiv:hep-ph/0701241](https://arxiv.org/abs/hep-ph/0701241).
- [25] M. Giordano and E. Meggiolaro, *J. High Energy Phys.* **03** (2014) 002.
- [26] V. V. Anisovich, V. A. Nikonov, and J. Nyiri, *Phys. Rev. D* **88**, 014039 (2013); **88**, 094015 (2013).
- [27] V. V. Anisovich, K. V. Nikonov, V. A. Nikonov, and J. Nyiri, *Int. J. Mod. Phys. A* **29**, 1450096 (2014).
- [28] V. V. Anisovich, M. A. Matveev, and V. A. Nikonov, [arXiv:1407.4588](https://arxiv.org/abs/1407.4588).
- [29] V. V. Anisovich, *AIP Conf. Proc.* **619**, 197 (2002); **717**, 441 (2004); *Usp. Fiz. Nauk* **47**, 49 (2004) [*Phys. Usp.* **47**, 45 (2004)].
- [30] V. V. Anisovich, M. A. Matveev, J. Nyiri, and A. V. Sarantsev, *Int. J. Mod. Phys. A* **20**, 6327 (2005).
- [31] G. Parisi and R. Petronzio, *Phys. Lett.* **94B**, 51 (1980).
- [32] M. Consoli and J. H. Field, *Phys. Rev. D* **49**, 1293 (1994).